ISSN 1674-1056
http://cpb.iphy.ac.cn
http://iopscience.iop.org/cpb
中国物理 B
Chinese Physics
中国物理
Chinese Physics B

Graphene-enhanced thermoelectric properties of p-type skutterudites

Dandan Qin(秦丹丹), Yuan Liu(刘媛), XianFu Meng(孟宪福), Bo Cui(崔博), Yaya Qi(祁亚亚), Wei Cai(蔡伟), Jiehe Sui(隋解和)
Citation: Chin. Phys. B . 2018, 27(4): 048402. **doi:** 10.1088/1674-1056/27/4/048402

Journal homepage: http://cpb.iphy.ac.cn; http://iopscience.iop.org/cpb

What follows is a list of articles you may be interested in

An ultra-wideband pattern reconfigurable antenna based on graphene coating

YanNan Jiang(姜彦南), Rui Yuan(袁锐), Xi Gao(高喜), Jiao Wang(王娇), SiMin Li(李思敏), Yi-Yu Lin(林诒玉)
Chin. Phys. B . 2016, 25(11): 118402. **doi:** 10.1088/1674-1056/25/11/118402

Biaxial strain-induced enhancement in the thermoelectric performance of monolayer WSe_2

Wanhuizi Shen(沈婉慧子), Daifeng Zou(邹代峰), Guozheng Nie(聂国政), Ying Xu(许英)
Chin. Phys. B . 2017, 26(11): 117202. **doi:** 10.1088/1674-1056/26/11/117202

Influences of spark plasma sintering temperature on the microstructures and thermoelectric properties of $(Sr_{0.95}Gd_{0.05})TiO_3$ ceramics

Li Liang-Liang, Qin Xiao-Ying, Liu Yong-Fei, Liu Quan-Zhen
Chin. Phys. B . 2015, 24(6): 067202. **doi:** 10.1088/1674-1056/24/6/067202

Probing the thermoelectric transport properties of n-type Bi_2Te_3 close to the limit of constitutional undercooling

Feng Song-Ke, Li Shuang-Ming, Fu Heng-Zhi
Chin. Phys. B . 2014, 23(11): 117202. **doi:** 10.1088/1674-1056/23/11/117202

Theoretical study of thermoelectric properties of MoS_2

Guo Huai-Hong, Yang Teng, Tao Peng, Zhang Zhi-Dong
Chin. Phys. B . 2014, 23(1): 017201. **doi:** 10.1088/1674-1056/23/1/017201

SPECIAL TOPIC — Recent advances in thermoelectric materials and devices

Graphene-enhanced thermoelectric properties of p-type skutterudites*

Dandan Qin(秦丹丹)[1], Yuan Liu(刘媛)[2,3], Xianfu Meng(孟宪福)[1], Bo Cui(崔博)[2], Yaya Qi(祁亚亚)[2], Wei Cai(蔡伟)[2], and Jiehe Sui(隋解和)[1,†]

[1] State Key Laboratory of Advanced Welding and Joining, Harbin Institute of Technology, Harbin 150001, China
[2] Department of Physics and TcSUH, University of Houston, Houston, Texas 77204, USA
[3] Fresenius Kabi USA, LLC, Melrose Park, IL 60160, USA

(Received 15 January 2018; revised manuscript received 8 March 2018; published online 29 March 2018)

Nanocomposite is proved to be an effective method to improve thermoelectric performance. In the present study, graphene is introduced into p-type skutterudite $La_{0.8}Ti_{0.1}Ga_{0.1}Fe_3CoSb_{12}$ by plasma-enhanced chemical vapor deposition (PECVD) method to form skutterudite/graphene nanocomposites. It is demonstrated that the graphene has no obvious effect on the electrical conductivity of $La_{0.8}Ti_{0.1}Ga_{0.1}Fe_3CoSb_{12}$, but the Seebeck coefficient is slightly improved at high temperature, thereby leading to high power factor. Furthermore, due to the enhancement of phonon scattering by the graphene, the lattice thermal conductivity is reduced significantly. Ultimately, the maximum zT value of $La_{0.8}Ti_{0.1}Ga_{0.1}Fe_3CoSb_{12}$/graphene is higher than that of graphene-free alloy and reaches to 1.0 at 723 K. Such an approach raised by us enriches prospects for future practical application.

Keywords: skutterudites, graphene, nanocomposites, thermoelectric properties

PACS: 84.60.Rb, 72.15.Jf, 77.84.Cg, 81.20.–n **DOI:** 10.1088/1674-1056/27/4/048402

1. Introduction

It is of great importance to develop clean and renewable energy sources due to the environmental pollution and resource shortage. Thermoelectric materials are most promising alternatives with the capacity of directly converting heat into useful electricity based on the Seebeck effect.[1,2] Despite the great success in the commercialized application in the space exploration,[3] the performance of thermoelectric devices is suffered from the low conversion efficiency. The thermoelectric conversion efficiency is mainly determined by the dimensionless figure of merit $zT = S^2\sigma T/\kappa$, where S is the Seebeck coefficient, σ is the electrical conductivity, T is the absolute temperature, κ is the total thermal conductivity composed of the lattice thermal conductivity κ_L and electronic thermal conductivity κ_e. Since the concept of phonon glasses and electron crystal was put forward, the filled skutterudites with high power factor, relative low thermal conductivity and excellent mechanical properties have been regarded as the promising mid-temperature TE materials.[4–6]

The filling elements, such as rare earth, alkali metals, alkali earth and other species,[7,8] into interstitial voids not only tune the carrier concentration by the donor doping, but also reduce the lattice thermal conductivity by strengthening the phonon scattering. Therefore, thermoelectric properties have been remarkably improved, especially for n-type skutterudites. The maximum zT value about 1.8 is obtained by adding $In_{0.4}Co_4Sb_{12}$ to triple-filled (Sr, Ba, Yb)$_y$Co$_4$Sb$_{12}$ and using high energy ball-milling method.[9] As high-performance thermoelectric devices, both p-type and n-type materials with high zT values are needed. However, the reported zT values of p-type filled skutterudites are lower than zT values of n-type skutterudites.[10–19] Therefore, development of zT values in p-type skutterudites remain challenging.

Nanocomposite is proved to be an effective method to improve the thermoelectric properties.[20–23] Carbon-based materials have been selected as a second phase to boost the thermoelectric properties. Shi *et al.*[24,25] reported the effect of fullerence (C_{60}) on the thermoelectric properties of $CoSb_3$ or Ba$_y$Co$_4$Sb$_{12}$. In such materials, the lattice thermal conductivity reduced due to the enhanced scattering of phonon. Feng *et al.*[26] fabricated the $CoSb_3$/graphene nanocomposite by an *in situ* solvothermal route combined with hot pressing, remarkable increasing zT value. Such an outstanding performance could be attributable to the reduced lattice thermal conductivity and remarkable increased power factor induced by the nanostructured matrix and the second phase incorporation. Wan *et al.*[27] found that the flexural strength and fracture toughness of the $CeFe_4Sb_{12}$ materials improved by introducing short carbon fibers while little impact on the thermoelectric performance. Zhang *et al.*[28] assembled SKDs with both single- and multi-walled carbon nanotubes via a cryogenic grinding technique to enhance the thermoelectric and

*Project supported by the National Natural Science Foundation of China (Grant Nos. 51622101, 51771065, and 51471061).
†Corresponding author. E-mail: suijiehe@hit.edu.cn
© 2018 Chinese Physical Society and IOP Publishing Ltd

mechanical properties. Recently, Zong *et al.*[29,30] reported the skutterudites-based composites by uniformly mixing the hydrophilic graphene oxide and skutterudites and followed by *in situ* reduction with spark plasma sintering. The result indicated that the introduction of graphene had minimal effect on the electrical properties, but evidently suppressed the lattice thermal conductivity, leading to enhanced figure merit of zT.

From this perspective, this study shows an improved zT value in skutterudites with the addition of graphene by plasma-enhanced chemical vapor deposition (PECVD) method. The purposely designed skutterudite/graphene nanocomposites exhibit higher Seebeck coefficient and lower lattice thermal conductivity than pure skutterudite.

2. Experiment section

2.1. Sample synthesis

High-purity elements of La ingot (99.9%, Alfa Aesar), Ti wire (99.9%, Alfa Aesar), Ga ingot (99.9999%, Alfa Aesar), Fe ingot (99.99%, Alfa Aesar), Co ingot (99.9%, Alfa Aesar), Sb balls (99.99%, Alfa Aesar) were weighted according to the stoichiometric ratio of $La_{0.8}Ti_{0.1}Ga_{0.1}Fe_3CoSb_{12}$. The mixture were put into the graphite crucible and then sealed in quartz tube under vacuum (10^{-3} Pa). The above procedures were operated in Ar-filled glove box. The sealed quartz tube was slowly heated to 1423 K and held for 3 h before quenching in water and then annealed at 973 K for 100 h in the muffle furnace. The obtained ingot was successively polished, cleaned, dried and finally ground into fine powders. The obtained powders were put into PECVD setup. Under flowing reaction gas mixtures (Ar:CH_4 = 90:50), the graphene grew on the surface of skutterudite powders with working pressure 500 Pa and radio frequency power 200 W at the temperature 600 °C for 30 min. The obtained composite powders were loaded in the graphite die with a diameter of 12.7 mm and hot-pressed at 923 K for 1 hour under the pressure of 90 MPa and vacuum of 5×10^{-3} Pa. Ultimately, high-densified bulk composite sample of $La_{0.8}Ti_{0.1}Ga_{0.1}Fe_3CoSb_{12}$/graphene was obtained. For comparison,the skutterudite sample was prepared by a similar route without the addition of graphene.

2.2. Sample characterization

The composition of skutterudite/graphenepowders was determined by Raman spectroscopy, and phase structure of bulk sample was analyzed by x-ray diffractometer (XRD) with a PANalytical X'Pert Pro using Cu–Kα radiation (λ = 1.5418 Å) and the scanning velocity of 3° per minute. The bars with dimension of 2 nm × 2 nm × 10 mm were prepared for the measurement of Seebeck coefficient and electrical conductivity from room temperature to 773 K under helium atmosphere on a device (CTA). The disks with diameter of 12.7 mm and thickness of 2 mm were used to measure the thermal diffusivity. The total thermal conductivity (κ) could be calculated using the relationship of $\kappa = D \times C_P \times \rho$, where D is thermal diffusivity evaluated from room temperature to 773 K with flowing argon gas on the Netzsch LFA457, C_P is specific heat determined using DSC system (Netzsch DSC 404), and ρ is density measured by the Archimedes method. The density of $La_{0.8}Ti_{0.1}Ga_{0.1}Fe_3CoSb_{12}$/graphene sample and graphene-free sample is 7.66 g/cm^3 and 7.65 g/cm^3, respectively. The relative densities of all samples are higher than 96%. The uncertainty for the electrical conductivity is 3%, the Seebeck coefficient is 5%, the thermal conductivity is 7%. So, the combined uncertainty for the power factor is 10% and that for zT value is ~12%.

3. Results and discussion

Figure 1 shows the Raman spectra of $La_{0.8}Ti_{0.1}Ga_{0.1}Fe_3CoSb_{12}$ and $La_{0.8}Ti_{0.1}Ga_{0.1}Fe_3CoSb_{12}$/graphene composite powders. Compared to graphene-free powders, it can be seen that two characteristic peaks of graphene are presented at 1340 cm^{-1} and 1580 cm^{-1} for composite powders, which are corresponded to the D and G peaks, respectively. This indicates that graphene is successfully grew on the surface of skutterudite powders by the PECVD method.

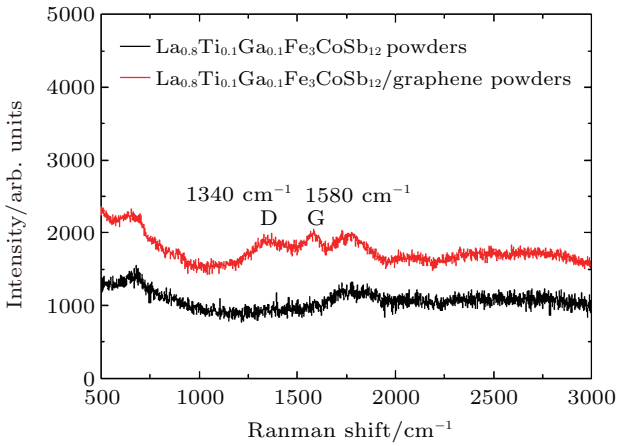


Fig. 1. (color online) Raman spectra of skutterudite and skutterudite/graphene composite powders.

Figure 2 shows the x-ray diffraction patterns of skutterudite/graphene composite. The peak located at 2θ around 26° indicates that a small amount of graphite phase occurred for the composites. From the results of Raman spectra and XRD, it can be concluded that the graphene is successfully introduced into skutterudite matrix. The lattice parameters of all samples determined by refined XRD data and the real filled fraction obtained via polyzonal EDS results are listed in Table 1. The similar lattice constant and real composition of both samples illustrate that the graphene is located in the boundary without causing the lattice distortion.

Figure 3 shows the temperature-dependent electrical properties of the $La_{0.8}Ti_{0.1}Ga_{0.1}Fe_3CoSb_{12}$/graphene sample and graphene-free sample. As shown in Fig. 3(a), the electrical conductivity σ shows similar values in the range of measurement temperature. Meanwhile, the electrical conductivity is decreased with increasing temperature for both samples, displaying typical degenerating semiconductor behavior.

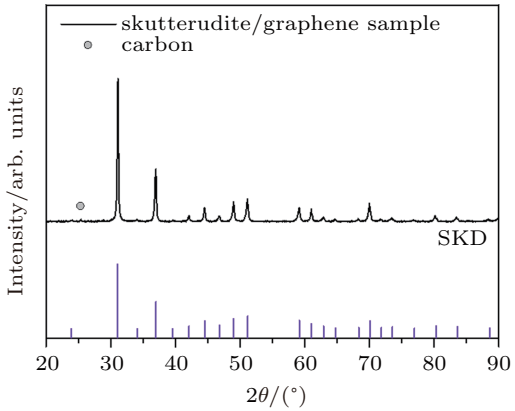


Fig. 2. (color online) XRD patterns of the sintered skutterudite/graphene sample.

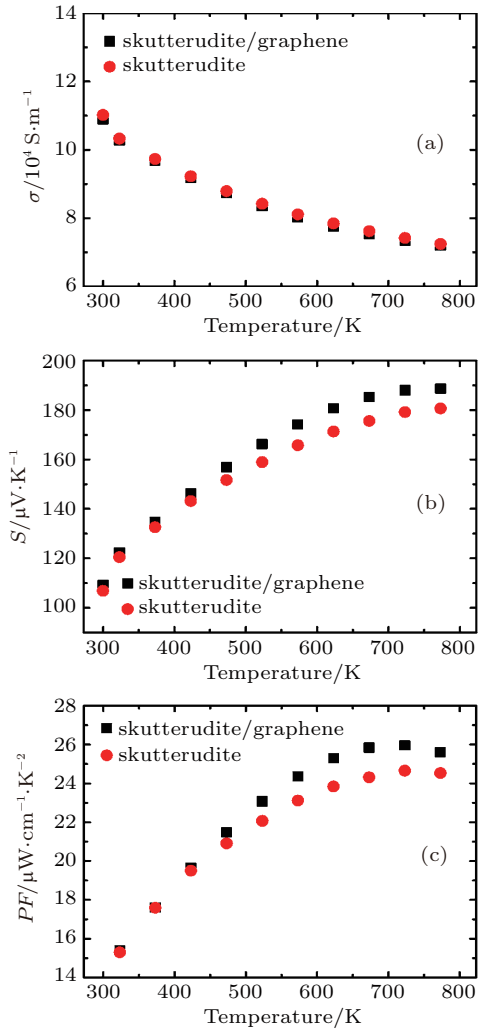


Fig. 3. (color online) Temperature-dependent electrical properties of skutterudite and skutterudite/graphene samples (a) electrical conductivity, (b) Seebeck coefficient, (c) powder factor.

Figure 3(b) shows the temperature-dependent of Seebeck coefficient for $La_{0.8}Ti_{0.1}Ga_{0.1}Fe_3CoSb_{12}$/graphene sample and graphene-free one. Both samples show positive value of Seebeck coefficient S, indicating p-type semiconductor. It is clearly seen that Seebeck coefficient keeps almost same below 473 K for both samples. However, for $La_{0.8}Ti_{0.1}Ga_{0.1}Fe_3CoSb_{12}$/graphene sample, the Seebeck coefficient is slightly higher than that of reference sample above 473 K.

Table 1. La actual filling fraction and lattice parameter for skutterudite/graphene and skutterudite.

Nominal composition	La (actual filling fraction)	Lattice parameter/Å
$La_{0.8}Ti_{0.1}Ga_{0.1}Fe_3CoSb_{12}$/graphene	0.68	9.110
$La_{0.8}Ti_{0.1}Ga_{0.1}Fe_3CoSb_{12}$	0.70	9.113

According to the above electrical conductivity and Seebeck coefficient, the power factors of the both samples are obtained using the relationship $PF = S^2\sigma$ as shown in Fig. 3(c). The $La_{0.8}Ti_{0.1}Ga_{0.1}Fe_3CoSb_{12}$/graphene sample shows the slightly improved power factor above 473 K due to the similar electrical conductivity and slightly enhanced Seebeck coefficient.

Figure 4 shows temperature-dependent thermal conductivity of $La_{0.8}Ti_{0.1}Ga_{0.1}Fe_3CoSb_{12}$/graphene sample and graphene-free sample. From Fig. 4(a), it can be seen that the total thermal coductivity κ for both samples has similar trend, which is first reduced and then increased with increasing temperature due to the Umklapp scattering and bipolar effect. Both samples have almost same thermal conductivity temperature below 373 K. However, the total thermal conductivity of $La_{0.8}Ti_{0.1}Ga_{0.1}Fe_3CoSb_{12}$/graphene sample is evidently lower than that of graphene-free one above 373 K. This interesting phenomenon is also same with the Seebeck coefficient. The electrical thermal conductivity κ_e is calculated by the Wiedemann–Franz law ($\kappa_e = L_0\sigma T$), where L_0 is the Lorentz numbers and often considered to be 2×10^{-8} $V^2 \cdot K^{-2}$.[31] The lattice thermal conductivity κ_L can be obtained by subtracting electronic thermal conductivity κ_e from κ. Figure 4(b) depicts the lattice thermal conductivity κ_L as a function of temperature for $La_{0.8}Ti_{0.1}Ga_{0.1}Fe_3CoSb_{12}$/graphene and graphene-free samples. Compared to reference sample, the $La_{0.8}Ti_{0.1}Ga_{0.1}Fe_3CoSb_{12}$/graphene sample has a lower lattice thermal conductivity. It can be considered that graphene introduced by PECVD method significantly reduces the lattice thermal conductivity due to the enhanced phonon scattering.

Figure 5 shows the temperature-dependent of zT value for the graphene and graphene-free skutterudite samples. While the temperature is below 523 K, the zT values of $La_{0.8}Ti_{0.1}Ga_{0.1}Fe_3CoSb_{12}$/graphene sample and the graphene-free one are comparable. However, the zT value of the

$La_{0.8}Ti_{0.1}Ga_{0.1}Fe_3CoSb_{12}$/graphene sample is significantly higher than that of reference sample above 523 K. The difference is consistent with the trend of Seebeck coefficient, power factor and lattice thermal conductivity. At 723 K, the maximum zT value of the $La_{0.8}Ti_{0.1}Ga_{0.1}Fe_3CoSb_{12}$/graphene sample is about 1.0 and increases by 25 % compared with graphene-free one.

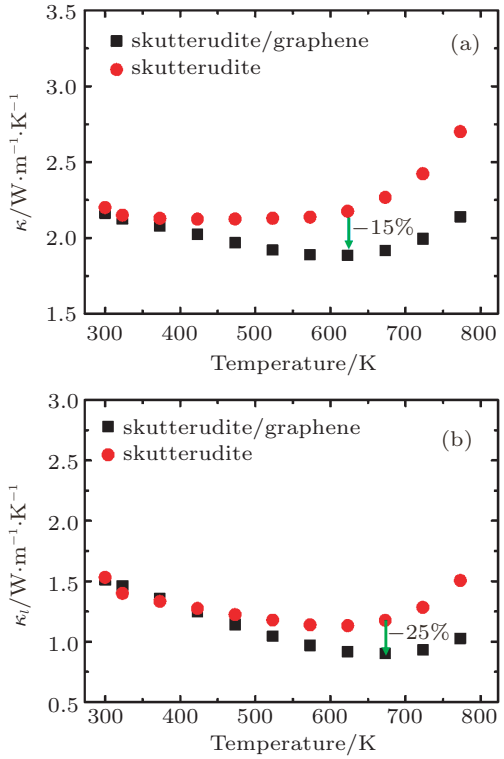


Fig. 4. (color online) Temperature-dependent thermal properties of skutterudite and skutterudite/graphene samples: (a) total thermal conductivity, (b) lattice thermal conductivity.

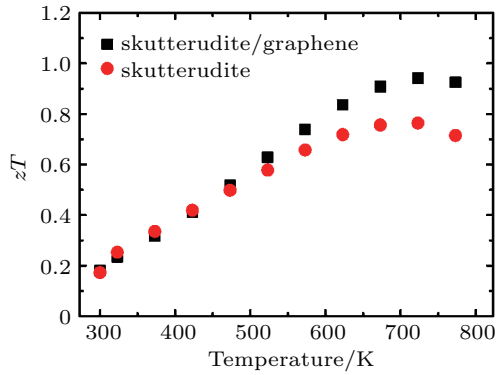


Fig. 5. (color online) Temperature-dependent zT values of skutterudite and skutterudite/graphene samples.

4. Conclusions

Graphene is successfully introduced into skutterudite by a PECVD method. The introduction of graphene has no obvious effect on the electrical conductivity of p-type $La_{0.8}Ti_{0.1}Ga_{0.1}Fe_3CoSb_{12}$ skutterudite, but remarkably enhanced Seebeck coefficient and decreased lattice thermal conductivity, leading to the high power factor and low total thermal conductivity especiallyat high temperature. Ultimately, the zT value is improved from 0.8 to 1.0 due to the addition of graphene.

References

[1] Chu S and Majumdar A 2012 *Nature* **488** 294
[2] Zhang Q H, Huang X Y, Bai S Q, Shi X, Uher C and Chen L D 2016 *Adv. Eng. Mater.* 2016 **18** 194
[3] Yang J and Caillat T 2006 *Mrs Bull.* **31** 224
[4] Rowe D M 1995 *CRC Handbook of Thermoelectrics* (New York: CRC Press)
[5] Sales B C, Mandrus D, Chakoumakos B C, Keppens V and Thompson J R 1997 *Phys. Rev. B* **56** 15081
[6] Rogl G and Rogl P 2017 *Current Opinion in Green and Sustainable Chemistry* **4** 50
[7] Keppens V, Mandrus D, Sales B C, Chakoumakos B C, Dai P, Coldea R, Maple M B, Gajewski D A, Freeman E J and Bennington S 1998 *Nature* **395** 876
[8] Sales B C 2003 *Handbook on the Physics & Chemistry of Rare Earths* **33** 1
[9] Rogl G, Grytsiv A, Yubuta K, Puchegger S, Bauer E, Raju C, Mallik R C and Rogl P 2015 *Acta Mater.* **95** 201
[10] Zhang L, Duan F, Li X, Yan X, Hu W, Wang L, Liu Z, Tian Y and Xu B 2013 *J. Appl. Phys.* **114** 083715
[11] Jie Q, Wang H, Liu W, Wang H, Chen G and Ren Z 2013 *Phys. Chem. Chem. Phys.* **15** 6809
[12] Dong Y, Nolas G S, Zeng X and Tritt T M 2015 *J. Mater. Res.* **30** 2558
[13] Guo L, Cai Z, Xu X, Peng K, Wang G, Wang G and Zhou X 2016 *Journal of Nanoscience & Nanotechnology* **16** 3841
[14] Lee W M, Shin D K and Kim I H 2015 *J. Electron. Mater.* **45** 1245
[15] Liu R, Qiu P, Chen X, Huang X and Chen L 2011 *J. Mater. Res.* **26** 1813
[16] Tan G J, Wang S Y and Tang X F 2014 *J. Electron. Mater.* **43** 1712
[17] Tang X, Zhang Q, Chen L, Goto T and Hirai T 2005 *J. Appl. Phys.* **97** 093712
[18] Rogl G, Grytsiv A, Heinrich P, Bauer E, Kumar P, Peranio N, Eibl O, Horky J, Zehetbauer M and Rogl P 2015 *Acta Materialia* **91** 227
[19] Dahal T, Jie Q, Liu W, Dahal K, Guo C, Lan Y and Ren Z 2015 *J. Alloys Compd.* **623** 104
[20] Rogl G, Grytsiv A, Failamani F, Hochenhofer M, Bauer E and Rogl P 2017 *J. Alloys Compd.* **695** 682
[21] Rogl G and Rogl P 2017 *Materials Today Physics* **3** 48
[22] Rogl G, Bursik J, Grytsiv A, Puchegger S, Soprunyuk V, Schranz W, Yan X, Bauer E and Rogl P 2018 *Acta Materialia* **145** 359
[23] Zhao W, Liu Z, Sun Z, Zhang Q, Wei P, Mu X, Zhou H, Li C, Ma S, He D, Ji P, Zhu W, Nie X, Su X, Tang X, Shen B, Dong X, Yang J, Liu Y and Shi J 2017 *Nature* **549** 247
[24] Shi X, Chen L D, Bai S Q, Huang X Y, Zhao X Y, Yao Q and Uher C 2007 *J. Appl. Phys.* **102** 103709
[25] Shi X, Chen L, Yang J and Meisner G P 2004 *Appl. Phys. Lett.* **84** 2301
[26] Feng B, Xie J, Cao G, Zhu T and Zhao X 2013 *J. Mater. Chem. A* **1** 13111
[27] Wan S, Huang X, Qiu P, Bai S and Chen L 2015 *Materials & Design* **67** 379
[28] Zhang Q, Zhou Z, Dylla M, Agne M T, Pei Y, Wang L, Tang Y, Liao J, Li J, Bai S, Jiang W, Chen L and Jeffrey Snyder G 2017 *Nano Energy* **41** 501
[29] Zong P A, Chen X, Zhu Y, Liu Z, Zeng Y and Chen L 2015 *J. Mater. Chem. A* **3** 8643
[30] Zong P A, Hanus R, Dylla M, Tang Y, Liao J, Zhang Q, Snyder G J and Chen L 2017 *Energy Environ. Sci.* **10** 183
[31] Shi X, Yang J, Salvador J R, Chi M, Cho J Y, Wang H, Bai S, Yang J, Zhang W and Chen L 2011 *J. Am. Chem. Soc.* **133** 7837